JOURNAL OF AIRCRAFT
Vol. 44, No. 2, March–April 2007

Cantilevered Plate Rayleigh–Ritz Trial Function Selection for von Kármán's Plate Equations

Peter J. Attar*
Computational Sciences Branch, Wright–Patterson Air Force Base, Ohio 45433-7913

DOI: 10.2514/1.25022

The accuracy and convergence characteristics of the classical Rayleigh–Ritz solution of the nonlinear von Kármán plate equations are studied with respect to the types of cantilever plate in-plane trial functions used in the solution. The static deflection of the cantilever plate is computed for an applied static gravity loading. Four different in-plane trial function types are studied. In each of these cases the same out-of-plane trial functions are used. It is found that in two of the four cases good convergence and accuracy are achieved when compared to the solution from a nonlinear finite element model. The degree of satisfaction of the problem natural boundary conditions is also examined, and it is shown that for the two cases that show inadequate convergence characteristics this satisfaction is poor. It is noted in particular that for these two cases at points on the problems' free boundaries, the in-plane trial functions satisfy, either exactly or approximately, the *linear* in-plane natural boundary conditions. At these points the addition of in-plane degrees of freedom to the solution will not contribute to the satisfaction of the *nonlinear* natural boundary condition. Thus for these two cases the convergence is poor as more in-plane trial functions are added to the solution. The change in the statically loaded plate natural frequencies are also computed. Similar to the static deflection results, convergence to the nonlinear finite element solution is slow when in-plane trial functions are used that approximately satisfy the linear in-plane boundary conditions.

I. Introduction

THE new breed of unmanned air vehicle/unmanned combat air vehicle (UAV/UCAV) configurations that are currently being developed will need to be highly maneuverable and fly at large angles of attack. This combination introduces the need for accurate, geometrically nonlinear structural models because large deflections and rotations will be involved. It is also true that whereas advances in computing power in recent years have allowed researchers and engineers to solve increasingly complex nonlinear problems using models with many degrees of freedom, the practical use of such models in design is still limited. Therefore reduced-order models (ROM) to nonlinear problems in structural mechanics are still being sought. The classical Rayleigh–Ritz (CRR) method is one such solution.

The Rayleigh–Ritz method is a procedure for the space discretization of distributed parameter systems. It was first developed by Lord Rayleigh in the 1870s for the study of vibration problems [1] and was extended by Ritz in 1909 to include multiple degrees of freedom for the approximating field [2,3]. In the Rayleigh–Ritz method, the approximating field is built with a set of trial functions that need only satisfy the following two conditions: 1) they need to be p times differentiable where p is the highest order, in the problem functional, of the spatial differential operator applied to the field variable that is being approximated, and 2) they need to satisfy all of the problem essential (kinematic) boundary conditions. It should be noted that the finite element method can be considered a Rayleigh–Ritz method in which the approximating functions are local functions defined only over subdomains of the geometry.

A question that arises when using the Rayleigh–Ritz method is the speed of convergence with respect to the number of functions used in the approximation. Meirovitch and Kwak [4] examined the convergence of the CRR method and the finite element method. In their work these methods were used to compute the eigenvalues of a nonuniform rod in axial vibration with one end fixed and the other restrained by a spring. They demonstrated that the convergence of the CRR method is greatly affected by the ability of the trial functions to satisfy the problem nonessential (natural) boundary conditions. By using a class of admissible functions called quasi-comparison functions they were able to markedly improve the convergence of the Rayleigh–Ritz method. The quasi-comparison functions are functions such that, whereas they alone do not satisfy the natural boundary conditions of the problem, finite linear combinations are able to satisfy them to any desired degree of accuracy. It was also noted in this work that in the finite element method, the rate of convergence is affected more by the ability of the trial functions to satisfy the differential equation than the boundary conditions.

The body of work on the nonlinear modeling of plates is extensive (see the literature reviews by Chia [5] and Sathyamoorthy [6]). Successful applications of nonlinear plate theory in the aerospace industry, specifically von Kármán's approximate small rotation version of nonlinear plate theory, include the computation of limit cycle oscillation (LCO) and buckling behavior of panels in supersonic flow [7–13].

With the recent increased interest in the modeling of highly flexible UAV/UCAV wings, the use of nonlinear plate and shell theory to model the response of fixed wing, cantilevered structures has also increased [14–24]. In work by Attar and Gordnier [21], LCO calculations were performed for a cropped delta wing planform and compared with those of a previous experiment [25]. The computations in this work used a finite element solution of a large rotation, nonlinear shell model. The LCO solutions were also compared with those from a previous work [22] that used a finite element solution of the small rotation, moderate deflection von Kármán plate equations. It was found that the LCO computed using finite element solutions of the von Kármán theory compared well with the large rotation model up to out-of-plane wingtip deflections of the order of $w/h \approx 15$ (where h is the model thickness). However in previous work by Attar et al. [18,19] it was noted that LCO results computed using a CRR solution of the von Kármán equations were poor when compared with experiment and a similar large rotation finite element model [19] and that convergence of the LCO results with respect to the number of in-plane functions used in the Rayleigh–Ritz solution was exceedingly slow [18].

In this paper the convergence characteristics, with respect to the in-plane trial functions, of the CRR solution of the von Kármán plate

Received 7 May 2006; revision received 26 June 2006; accepted for publication 5 July 2006.

*NRC Fellow; peter.attar@wpafb.af.mil.

equations will be studied for the static displacement of a cantilevered plate. Various types of trial functions will be used in the expansion of the in-plane displacements and it will be shown that convergence of the solution is greatly dependent on the ability of the trial functions to accurately satisfy the nonessential (natural) boundary conditions of the problem.

II. Theoretical Development

In this section an overview will be given of the development of the von Kármán plate equations. For a more detailed analysis of nonlinear plate theory, please see the book by Novozhilov [26]. For a more detailed discussion of the von Kármán version of nonlinear plate theory, please see the book by Dowell [27].

The general geometrically exact, strain-displacement relationships can be written in terms of the displacements u, v, and w in the following manner:

$$\varepsilon_{xx} = u_x + \frac{1}{2}\left(u_x^2 + v_x^2 + w_x^2\right) \tag{1}$$

$$\varepsilon_{yy} = v_y + \frac{1}{2}\left(u_y^2 + v_y^2 + w_y^2\right) \tag{2}$$

$$\varepsilon_{zz} = w_z + \frac{1}{2}\left(u_z^2 + v_z^2 + w_z^2\right) \tag{3}$$

$$\varepsilon_{xy} = u_y + v_x + u_x u_y + v_x v_y + w_x w_y \tag{4}$$

$$\varepsilon_{xz} = (1 + u_x)u_z + v_x v_z + w_x(1 + w_z) \tag{5}$$

$$\varepsilon_{yz} = u_y u_z + (1 + v_y)v_z + w_y(1 + w_z) \tag{6}$$

This is the Green form of the strain-displacement relationships and it imposes no restrictions on the magnitude of elongations, shears, or rotation.

The basic assumptions used in the theory of thin plates are attributed to Kirchhoff. The assumptions are [26] 1) every point of the plate remains, after deformation, on the same perpendicular to the middle surface as before deformation, and 2) the distance of every point of the plate from the middle surface remains unchanged by the deformation. These assumptions can be expressed by the following differential equations:

$$\varepsilon_{xz} = (1 + u_x)u_z + v_x v_z + w_x(1 + w_z) = 0 \tag{7}$$

$$\varepsilon_{yz} = u_y u_z + (1 + v_y)v_z + w_y(1 + w_z) = 0 \tag{8}$$

$$\varepsilon_{zz} = w_z + \frac{1}{2}(u_z^2 + v_z^2 + w_z^2) = 0 \tag{9}$$

Solutions to Eqs. (7–9) can be written as

$$u = \hat{u} + z\vartheta(x, y) \tag{10}$$

$$v = \hat{v} + z\psi(x, y) \tag{11}$$

$$w = \hat{w} + z\chi(x, y) \tag{12}$$

where $\hat{u}$, $\hat{v}$, and $\hat{w}$ are midplane displacements. Choosing solutions of the type given in Eqs. (10–12) is equivalent to looking for a solution to Eqs. (7–9) in the form of a power series in z and only retaining the first two terms.

The Kirchhoff assumptions make it possible to write the strain purely in terms of the midplane displacements, $\hat{u}$, $\hat{v}$, and $\hat{w}$. To do this, first the expressions for u, v, and w from Eqs. (10–12) are placed into Eqs. (7–9) and the assumption is made that the plate elongations and shears are small compared to unity. This results in the following expressions for ϑ, ψ, and χ:

$$\vartheta \approx -\hat{w}_x(1 + \hat{v}_y) + \hat{v}_x\hat{w}_y \tag{13}$$

$$\psi \approx -\hat{w}_y(1 + \hat{u}_x) + \hat{u}_y\hat{w}_x \tag{14}$$

$$\chi \approx \hat{u}_x + \hat{v}_y + \hat{u}_x\hat{v}_y - \hat{u}_y\hat{v}_x \tag{15}$$

Note that requiring that elongations and shears be small compared to unity is often called small strain theory and it places no limit on the magnitude of the rotations. Finally if Eqs. (13–15) are then placed into Eqs. (10–12) and the resulting expressions are then placed into Eqs. (1), (2), and (4), equations for the strains ε_{xx}, ε_{yy}, and ε_{xy} entirely in terms of the midplane displacements are found. Because a simplified version of nonlinear plate theory will be used in this work, these expressions will not be shown here.

If the angles of rotation of the elements of a plate can be considered small in comparison to unity, further assumptions can be made to simplify the strain-displacement relationships. Namely, all terms that are nonlinear in the derivatives of the midplane in-plane displacements (i.e., terms like $\hat{u}_x^2$, $\hat{u}_y\vartheta_x$, etc.) can be neglected. These are the assumptions that are used in the von Kármán version of nonlinear plate theory. With these simplifications the strain terms ε_{xx}, ε_{yy}, and ε_{xy} can be then written as

$$\varepsilon_{xx} = \tilde{\varepsilon}_{xx} + z\hat{\kappa}_{xx} \tag{16}$$

$$\varepsilon_{yy} = \tilde{\varepsilon}_{yy} + z\hat{\kappa}_{yy} \tag{17}$$

$$\varepsilon_{xy} = \tilde{\varepsilon}_{xy} + z\hat{\kappa}_{xy} \tag{18}$$

where

$$\tilde{\varepsilon}_{xx} = \hat{u}_x + \frac{1}{2}\left(\hat{w}_x^2\right) \tag{19}$$

$$\tilde{\varepsilon}_{yy} = \hat{v}_y + \frac{1}{2}\left(\hat{w}_y^2\right) \tag{20}$$

$$\tilde{\varepsilon}_{xy} = \hat{u}_y + \hat{v}_x + \hat{w}_x\hat{w}_y \tag{21}$$

$$\hat{\kappa}_{xx} = \vartheta_x \approx -\hat{w}_{xx} \tag{22}$$

$$\hat{\kappa}_{yy} = \psi_y \approx -\hat{w}_{yy} \tag{23}$$

$$\hat{\kappa}_{xy} = \vartheta_y + \psi_x \approx -2\hat{w}_{xy} \tag{24}$$

With the degree of accuracy given by the preceding approximations, the displacements of the points of the plate can be written as

$$u = \hat{u} - z\hat{w}_x \tag{25}$$

$$v = \hat{v} - z\hat{w}_y \tag{26}$$

$$w = \hat{w} \tag{27}$$

For a linear elastic, isotropic material the stress-strain relationships are

$$\sigma_{xx} = \frac{E}{(1-\nu^2)}(\varepsilon_{xx} + \nu\varepsilon_{yy}) \tag{28}$$

$$\sigma_{yy} = \frac{E}{(1-\nu^2)}(\varepsilon_{yy} + \nu\varepsilon_{xx}) \tag{29}$$

$$\sigma_{xy} = G\varepsilon_{xy} \tag{30}$$

and the elastic energy is given by

$$U = \frac{1}{2}\iiint (\sigma_{xx}\varepsilon_{xx} + \sigma_{yy}\varepsilon_{yy} + \sigma_{xy}\varepsilon_{xy})\,\mathrm{d}x\,\mathrm{d}y\,\mathrm{d}z \tag{31}$$

If the following definitions are made,

$$N_x = \int \sigma_x\,\mathrm{d}z \tag{32}$$

$$N_y = \int \sigma_y\,\mathrm{d}z \tag{33}$$

$$N_{xy} = \int \sigma_{xy}\,\mathrm{d}z \tag{34}$$

and Eqs. (16–25), (29), and (30) are taken into account, the following expressions for the membrane stress resultants N_x, N_y, and N_{xy} can be written in terms of the midplane displacements:

$$N_x = \frac{Eh}{(1-\nu^2)}(\tilde{\varepsilon}_{xx} + \nu\tilde{\varepsilon}_{yy}) = \frac{Eh}{(1-\nu^2)}\left[\hat{u}_x + \nu\hat{v}_y + \frac{1}{2}\left(\hat{w}_x^2 + \nu\hat{w}_y^2\right)\right] \tag{35}$$

$$N_y = \frac{Eh}{(1-\nu^2)}(\tilde{\varepsilon}_{yy} + \nu\tilde{\varepsilon}_{xx}) = \frac{Eh}{(1-\nu^2)}\left[\hat{v}_y + \nu\hat{u}_x + \frac{1}{2}\left(\hat{w}_y^2 + \nu\hat{w}_x^2\right)\right] \tag{36}$$

$$N_{xy} = Gh\tilde{\varepsilon}_{xy} = Gh(\hat{u}_y + \hat{v}_x + \hat{w}_x\hat{w}_y) \tag{37}$$

If the expressions for ε_{xx}, ε_{yy}, ε_{xy} from Eqs. (16–18) are used along with Eqs. (28–30), after integration from $z = -\frac{1}{2}h$ to $z = \frac{1}{2}h$, an expression for the strain energy U can be written in terms of the midplane displacements:

$$\begin{aligned} U = {} & \frac{Eh}{2(1-\nu^2)}\iint\left[\left(\hat{u}_x + \frac{1}{2}\hat{w}_x^2\right)^2 + \left(\hat{v}_y + \frac{1}{2}\hat{w}_y^2\right)^2 + 2\nu\left(\hat{u}_x + \frac{1}{2}\hat{w}_x^2\right)\left(\hat{v}_y + \hat{w}_y^2\right) + \frac{(1-\nu)}{2}(\hat{v}_x + \hat{u}_y + \hat{w}_x\hat{w}_y)^2\right]\mathrm{d}x\,\mathrm{d}y \\ & + \frac{D}{2}\iint\left[\hat{w}_{xx}^2 + \hat{w}_{yy}^2 + 2\nu\hat{w}_{xx}\hat{w}_{yy} + 2(1-\nu)\hat{w}_{xy}^2\right]\mathrm{d}x\,\mathrm{d}y \end{aligned} \tag{38}$$

where $D = Eh^3/12(1-\nu^2)$. In Eq. (38) the first integral is the strain energy due to stretching, whereas the second integral is the strain energy due to bending.

In this paper the only external loading considered will be an static load in the form of gravity in the out-of-plane direction. Therefore the total potential energy functional of the system in question can be written as the sum of the strain energy and gravitational potential energy:

$$V = U + h\iint \rho_m\hat{w}g\,\mathrm{d}x\,\mathrm{d}y \tag{39}$$

where ρ_m is the mass per unit area of the plate.

To derive the differential equations of motion and the problem nonessential boundary conditions, the first variation in the potential energy functional V is taken. Although the final form of the differential equations of motion will not be shown here (see, for example, [27]), the boundary conditions will be shown because they will be discussed in the results section. For a rectangular plate with an x dimension a and a y dimension b, the following boundary conditions are identified:

$\hat{u}$ equation:

$$\begin{aligned} &N_x = 0 \quad \text{or} \quad \hat{u} \text{ specified on } x = 0, a \\ &N_{xy} = 0 \quad \text{or} \quad \hat{u} \text{ specified on } y = 0, b \end{aligned} \tag{40}$$

$\hat{v}$ equation:

$$\begin{aligned} &N_{xy} = 0 \quad \text{or} \quad \hat{v} \text{ specified on } x = 0, a \\ &N_y = 0 \quad \text{or} \quad \hat{v} \text{ specified on } y = 0, b \end{aligned} \tag{41}$$

$\hat{w}$ equation:

$$\begin{aligned} &D(\hat{w}_{xx} + \nu\hat{w}_{yy}) = 0 \quad \text{or} \quad \hat{w}_x \text{ specified on } x = 0, a \\ &-D[\hat{w}_{xxx} + (2-\nu)\hat{w}_{xyy}] + N_x\hat{w}_x + N_{xy}\hat{w}_y = 0 \quad \text{or} \\ &\quad \hat{w} \text{ specified on } x = 0, a \\ &D(\hat{w}_{yy} + \nu\hat{w}_{xx}) = 0 \quad \text{or} \quad \hat{w}_y \text{ specified on } y = 0, b \\ &-D[\hat{w}_{yyy} + (2-\nu)\hat{w}_{xxy}] + N_y\hat{w}_y + N_{xy}\hat{w}_x = 0 \quad \text{or} \\ &\quad \hat{w} \text{ specified on } y = 0, b \\ &D2(1-\nu)\hat{w}_{xy} = 0 \quad \text{or} \quad \hat{w} \text{ specified on } x = 0, a \quad \text{and} \quad y = 0, b \end{aligned} \tag{42}$$

In the Rayleigh–Ritz solution, procedure expressions for $\hat{u}$, $\hat{v}$, and $\hat{w}$ are written in the following manner:

$$\hat{u} = \sum_{i=1}^{mxy} a_i\phi_i(x, y) \tag{43}$$

$$\hat{v} = \sum_{i=1}^{mxy} b_i\eta_i(x, y) \tag{44}$$

$$\hat{v} = \sum_{i=1}^{nxy} q_i\beta_i(x, y) \tag{45}$$

and placed into Eq. (39) using Eq. (38). As was mentioned in the introduction, the functions ϕ_i, η_i, and β_i must be of the admissible type, that is, they must satisfy all geometric boundary conditions [conditions placed on $\hat{u}$, $\hat{v}$, $\hat{w}$, $\hat{w}_x$, and $\hat{w}_y$ in Eqs. (40–42)] and must be p times differentiable. Examining Eq. (38), p here is 1 for $\hat{u}$ and $\hat{v}$ and 2 for $\hat{w}$. In the CRR solution method, the trial functions $\phi_i(x, y)$, $\eta_i(x, y)$, and $\beta_i(x, y)$ span the entire spatial domain. The principle of stationary potential energy then states that the equilibrium configuration for the structure is defined by the $2 * mxy + nxy$ algebraic equations which result from making the potential energy V stationary with respect to the a_i, b_i, and q_i:

$$\frac{\partial V}{\partial a_i} = 0 \qquad i = 1, mxy \tag{46}$$

$$\frac{\partial V}{\partial b_i} = 0 \qquad i = 1, mxy \tag{47}$$

$$\frac{\partial V}{\partial q_i} = 0 \qquad i = 1, nxy \tag{48}$$

Solving the algebraic equations defined by Eqs. (46–48) for the unknown a_i, b_i, and q_i results in the displacement fields $\hat{u}$, $\hat{v}$, and $\hat{w}$ being completely defined. In the von Kármán form of the nonlinear plate equations, the resulting set of algebraic equations is linear in the generalized displacements a_i and b_i and nonlinear in the q_i. See [27] for the final form of these equations.

After the expansions of u, v, and w are inserted into Eq. (38) the coefficients in Eq. (38) are functions of the derivatives of the trial functions. In this work these derivatives are computed using second-order finite differences. A trapezoid rule is used for the integration over the plate area in Eq. (38). The grid used to do these computations was a 21×21. A Newton–Raphson procedure is used to solve the nonlinear algebraic equations.

III. Results

In this work the static deflection of a square, cantilevered plate is studied. A static gravity loading is applied to the plate. The plate has dimension of 1×1 m and has a constant thickness of 0.001 m. The plate material properties are an elastic modulus of $3.3e^9$ N/m^2, a density of 1299 kg/m^3, and a Poisson ratio of 0.45. The plate is clamped along the edge $x = 0, 1$, $y = 0$, with zero out-of-plane and in-plane displacements and zero rotation along this edge.

For all of the cases presented in this section, the trial functions [the $\beta_i(x, y)$ in Eq. (45)] used to expand the out-of-plane deflections are the same. These were calculated using a finite element modal analysis of the cantilevered plate. Also the number of out-of-plane trial functions [nxy in Eq. (45)] is 10 for all of the results shown.

Results for four CRR solutions will be given here, each having different in-plane trial functions. Each of these trial functions satisfy the in-plane essential boundary conditions, which for this cantilevered plate problem are that $u = v = 0$ at $x = 0, 1$ $y = 0$.

1) The results labeled "CRR polynomial" have trial functions, which are polynomials and are generated in the following manner:

$$\begin{aligned} u(\xi, \eta) &= \psi_b(\xi, \eta) \sum_{n=0}^{m} \sum_{r=0}^{q} a_i \zeta_i(\xi, \eta) \\ v(\xi, \eta) &= \psi_b(\xi, \eta) \sum_{n=0}^{m} \sum_{r=0}^{q} b_i \zeta_i(\xi, \eta) \qquad \zeta_i(\xi, \eta) = \xi^r \eta^{q-r} \end{aligned} \tag{49}$$

where m is the degree of a two-dimensional polynomial, the coordinates ξ and η are x/a and y/b, respectively, and the number of terms in the expansion is $[(m + 1)(m + 2)]/2$. The function $\psi_b(\xi, \eta)$ is a boundary polynomial used to enforce the essential boundary conditions. Here this function is $\psi_b(\xi, \eta) = \eta$. See [28] for more details on the use of simple polynomials in CRR solutions.

2) The results labeled "CRR in-plane eigenmodes" use in-plane trial functions, which are the in-plane eigenmodes of the plate as calculated using a plane stress finite element model. The shape functions used in this finite element model are the standard bilinear quadrilateral type. The in-plane trial functions used in this case are different for u and v.

3) The results labeled "CRR out-of-plane eigenmodes" use in-plane trial functions generated using the *out-of-plane* modes for a plate simply supported at $x = 0, 1$, $y = 0$ as calculated using a finite element model constructed of shell elements.

4) The final set of classic Rayleigh–Ritz results, labeled, "CRR transcendental," are generated using products of sines and cosines in the following manner:

$$u(\xi, \eta) = \sum_{i=1}^{NX} \sum_{j=1}^{NY} a_{ij} \alpha_i(\xi) \beta_j(\eta) \tag{50}$$

$$v(\xi, \eta) = \sum_{i=1}^{NX} \sum_{j=1}^{NY} b_{ij} \alpha_i(\xi) \beta_j(\eta) \tag{51}$$

$$\alpha_i(\xi) = 2 \qquad i = 1 \qquad \alpha_i(\xi) = \cos(i\pi\xi) \qquad i = 2, NX \tag{52}$$

$$\beta_j(\eta) = \sin[(j - 0.50)\pi\eta] \qquad j = 1, NY \tag{53}$$

The functions α_i and β_j in Eqs. (52) and (53) are the eigenmodes for a free-free and clamped-free uniform rod in axial vibration, respectively. For the results presented in this work, the value of NX in Eqs. (50) and (51) is fixed at 8 and NY is varied from 1 to 12.

Figures 1–4 are plots of the convergence of the normalized out-of-plane (w/h) and in-plane (v/h) displacements with respect to the number of trial functions (mxy) used in Eqs. (43) and (44). Also shown in these figures is the result from a nonlinear, large rotation finite element model with 400 shell elements. In these figures it is obvious that the CRR polynomial and CRR out-of-plane results are much better than those of the other two cases. The converged displacements, both w/h and v/h, are within 0.3% of the finite element method (FEM) result and convergence to the result is very quick with less than 40 trial functions needed. See Figs. 5–7 for contour plots of the u, v, and w displacements for the converged CRR polynomial solution for $mxy = 36$. On the other hand, the other two

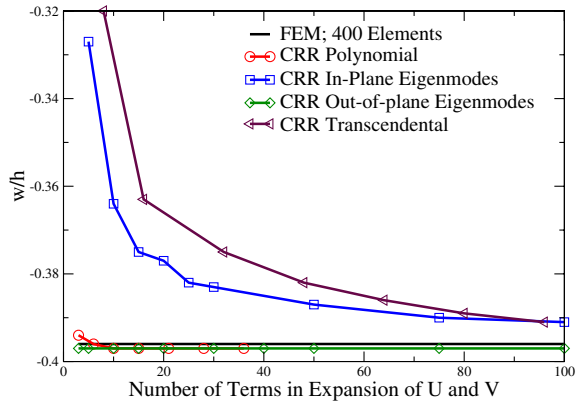

Fig. 1 Convergence of the out-of-plane deflection for a static gravity loading of 0.00078125 m/s^2.

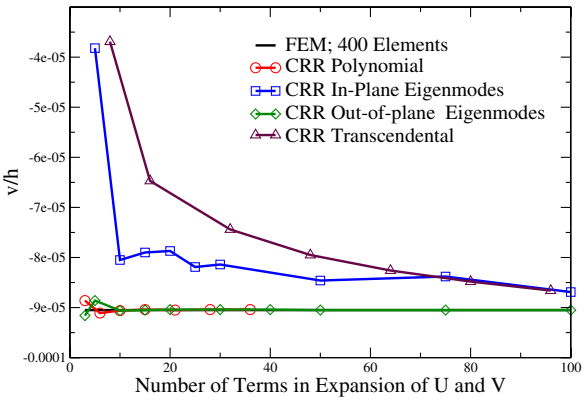

Fig. 2 Convergence of the in-plane deflection v for a static gravity loading of 0.00078125 m/s^2.

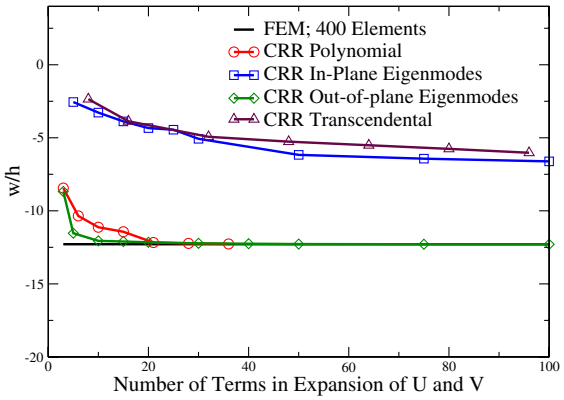

Fig. 3 Convergence of the out-of-plane deflection for a static gravity loading of 0.025 m/s^2.

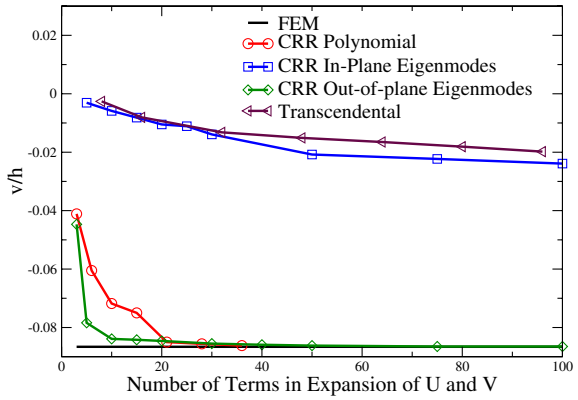

Fig. 4 Convergence of the in-plane deflection v for a static gravity loading of 0.025 m/s^2.

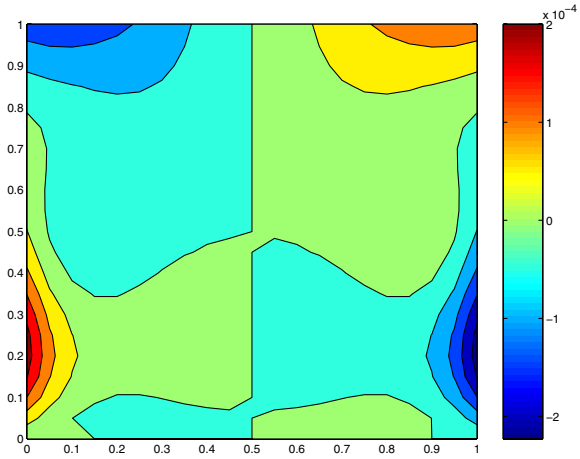

Fig. 5 Contours of u for the CRR polynomial case; static gravity load of 0.025 m/s^2.

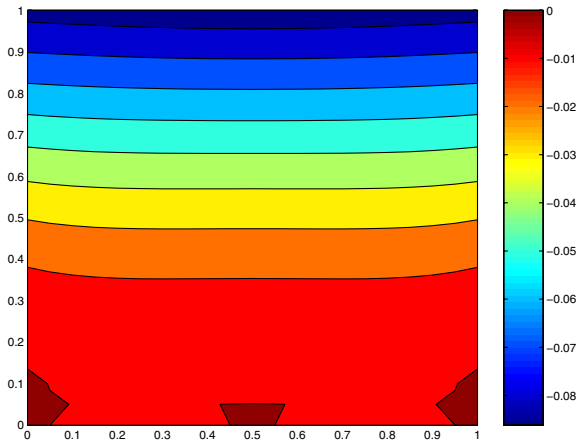

Fig. 6 Contours of v for the CRR polynomial case; static gravity load of 0.025 m/s^2.

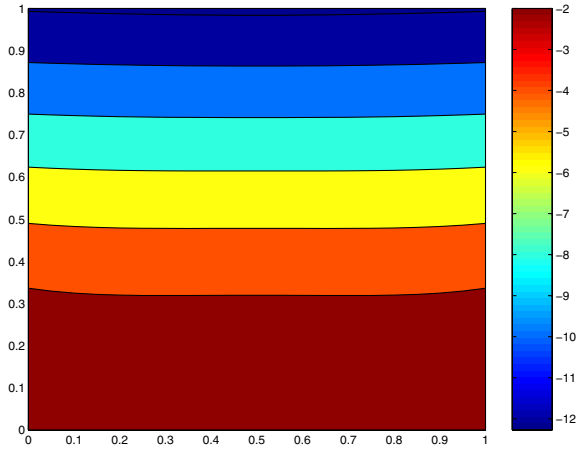

Fig. 7 Contours of w for the CRR polynomial case; static gravity load of 0.025 m/s^2.

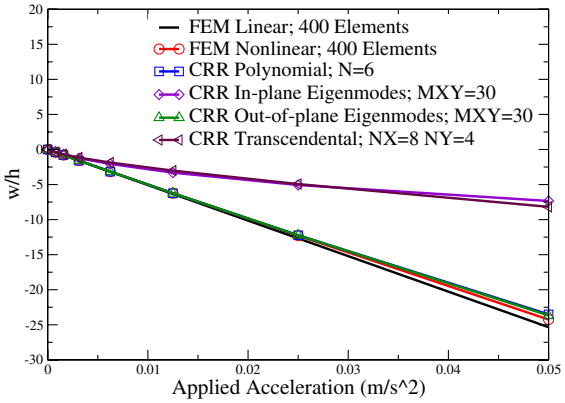

Fig. 8 w/h vs applied static gravity loading for the CRR solutions and FEM.

models, CRR in-plane eigenmodes and CRR transcendental, both show poor convergence. In Figs. 1 and 2, both cases are within 2% of the FEM result, but at least $mxy = 80$ trial functions are needed to achieve this accuracy. For Figs. 3 and 4, the error in the result is still over 40% for $mxy > 80$. In Figs. 8 and 9 the normalized out-of-plane (w/h) and y in-plane (v/h) deflections are plotted vs static gravity loading for the various CRR solutions at a fixed number of in-plane trial functions (as denoted in the figures). Also shown are the finite element solutions for a 400-element model. One can see that the CRR polynomial and CRR out-of-plane eigenmodes cases compare favorably with the finite element solution over the range of loadings used in the computation. However, the CRR in-plane eigenmodes and CRR transcendental cases show large errors even for normalized out-of-plane displacements on the order of 1 plate thickness.

So the question that now must be answered is why there is such a large disparity in the convergence and accuracy of the various results. As was mentioned earlier, all of the in-plane trial functions used here satisfy the problem essential boundary conditions, which is the only requirement on the trial functions (other than differentiability, which is also satisfied) for the Rayleigh–Ritz procedure. However, the ability of these trial functions to satisfy the problem differential equations and natural boundary conditions does vary substantially, as will be shown. Shown in Figs. 10 and 11 are the membrane stress

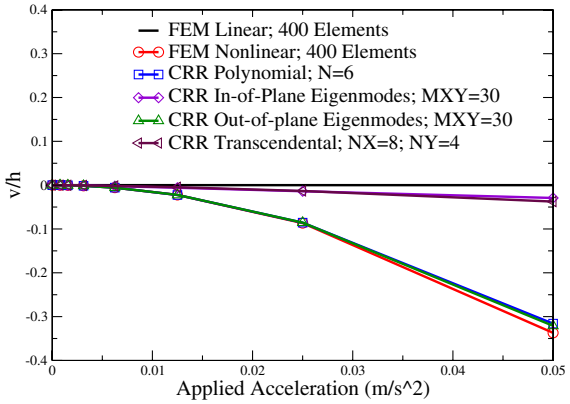

Fig. 9 v/h vs applied static gravity loading for the CRR solutions and FEM.

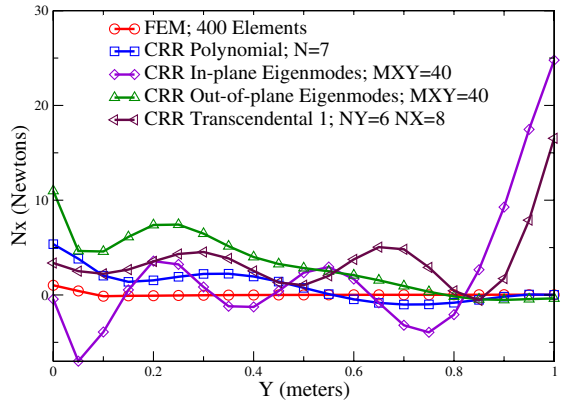

Fig. 10 Stress resultant Nx vs y at $x = 0.0$.

resultants Nx and Ny plotted vs y and x, respectively. In Fig. 10 the values of Nx are for $x = 0$, and in Fig. 11 the values of Ny are for $y = 1$. Because these are free edges, in Fig. 10 Nx should be zero for $x = 0$, $y > 0$ and in Fig. 11 Ny should be zero for all x. In these figures, results from the four CRR solutions are plotted along with the nonlinear finite element result. In Fig. 10 it appears that all of the CRR solutions do not satisfy the natural boundary conditions as well as the finite element solution. It does appear that for the two cases that show good convergence with respect to the number of in-plane trial, CRR polynomial and CRR out-of-plane eigenmodes, Nx approaches zero as y goes to 1. In the other two cases, the error in Nx grows as y goes to 1. In Fig. 11, the CRR polynomial and CRR out-of-plane eigenmodes cases approximately satisfy the $Ny = 0$ condition, whereas the other two cases have large errors. The errors in Ny for the CRR transcendental case can be explained in the following manner. For the boundary condition on Ny to be satisfied at $y = 1$, it follows

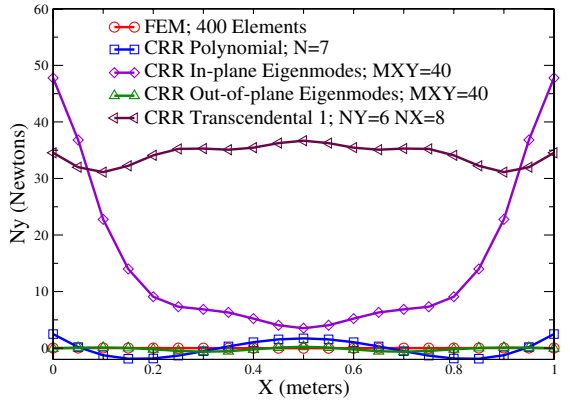

Fig. 11 Stress resultant Ny vs x at $y = 1.0$.

from Eqs. (36), (50), and (51) that the following statement must be true:

$$\nu \sum_{i=2}^{NX} \sum_{j=1}^{NY} [-a_{ij} i\pi \sin(i\pi x)(-1)^{j-1}] + \frac{1}{2}\left(w_y^2 + \nu w_x^2\right) = 0 \qquad (54)$$

where the expansion of the out-of-plane deflection w in its trial functions has not been written explicitly. In examining Eq. (54), it is obvious that at $x = 0$ and $x = 1$, this expression cannot be satisfied unless the out-of-plane contribution to Ny $(w_y^2 + \nu w_x^2)$, goes to zero. In essence the solution is "locked" with respect to the in-plane trial functions in that adding more in-plane degrees of freedom will not improve the solution with respect to the satisfaction of the natural boundary conditions at $x = 0$, $y = 1$ and $x = 1$, $y = 1$. This locking occurs due to the fact that at $x = 0$, $y = 1$ and $x = 1$, $y = 1$, the trial functions exactly satisfy the linear Ny stress resultant boundary condition of

$$Ny = \frac{Eh}{(1-\nu^2)}(\hat{v}_y + \nu \hat{u}_x) = 0 \qquad (55)$$

Figures 12–14 are plots of the in-plane $\{[Eh/(1-\nu^2)](\hat{v}_y + \nu\hat{u}_x)\}$ and out-of-plane $\{[Eh/(1-\nu^2)][\frac{1}{2}(\hat{w}_y^2 + \nu\hat{w}_x^2)]\}$ contributions to the Ny stress resultant vs x at $y = 1$ for the CRR polynomial, CRR in-plane eigenmodes, and CRR transcendental cases. One can see the locking effect for both the CRR in-plane eigenmodes and CRR transcendental case. Once again, the reason that the CRR in-plane eigenmodes case also locks is due to the approximate satisfaction at $y = 1$ of the linear Ny stress resultant boundary condition when the eigenmodes are computed using a linear plane stress finite element model. Note that refining the mesh used in the calculation of the in-plane eigenmodes for the CRR in-plane eigenmodes case will only make the locking worse because the refinement will improve the

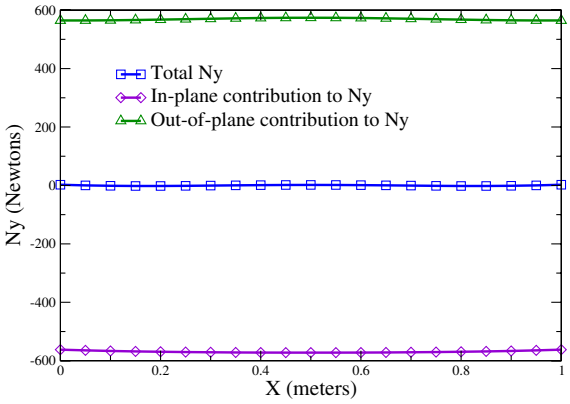

Fig. 12 In-plane, out-of-plane, and total Ny vs x for $y = 1$ and CRR polynomial case.

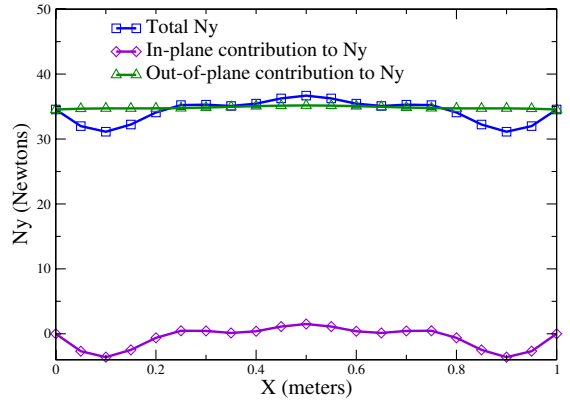

Fig. 13 In-plane, out-of-plane, and total Ny vs x for $y = 1$ and CRR transcendental case.

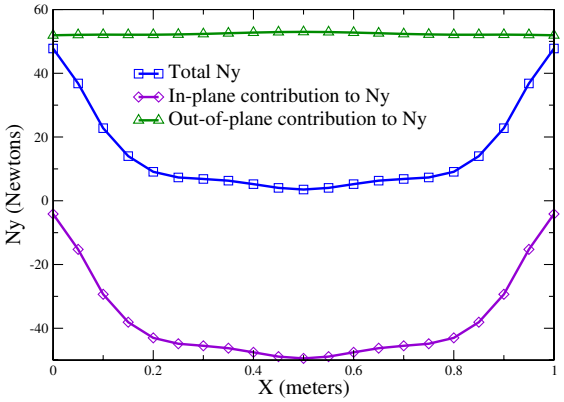

Fig. 14 In-plane, out-of-plane, and total *Ny* vs *x* for $y = 1$ and CRR in-plane eigenmodes case.

satisfaction of the linear membrane stress resultant boundary conditions. On the other hand, in Fig. 12 the locking phenomena is not evident, as there are no a priori conditions on $(\hat{v}_y + \nu\hat{u}_x)$ and all of the degrees of freedom are available to satisfy the natural boundary conditions. This is also true for the CRR out-of-plane eigenmodes case, and no locking occurs for this choice of in-plane trial functions as well.

The flutter characteristics of a loaded wing is of great interest to those who design aircraft. Because the flutter behavior of a wing is dependent on the structural natural frequencies, it is important to accurately predict the change in these quantities due static deflection, which occurs due to geometric nonlinearity. Shown in Figs. 15–18 are the plots of the first four natural frequencies as a function of the number of trial functions used for u and v for the CRR in-plane eigenmodes and CRR out-of-plane eigenmodes cases. The load applied to the plate to create a static deflection was a static gravity load of 0.05 $\mathrm{m/s^2}$ (results in a maximum w/h of 24.25). To compute

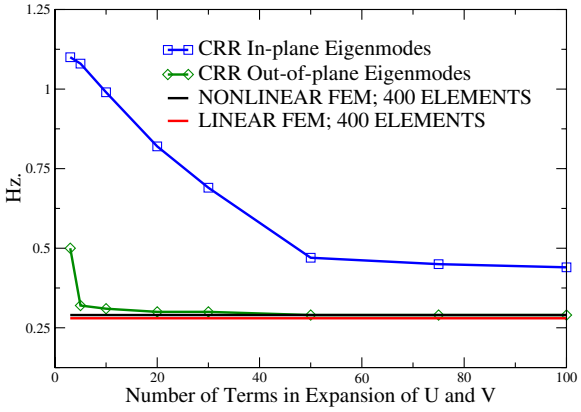

Fig. 15 Convergence of the plate first natural frequency.

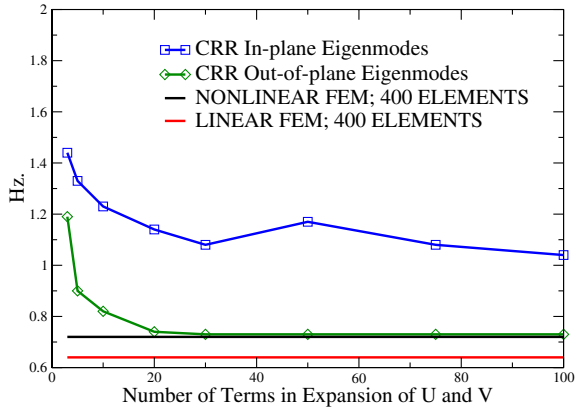

Fig. 16 Convergence of the plate second natural frequency.

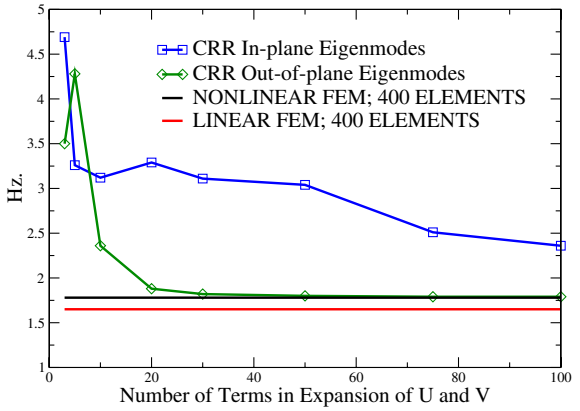

Fig. 17 Convergence of the plate third natural frequency.

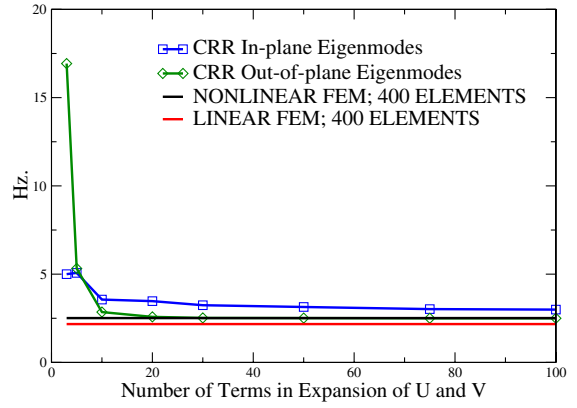

Fig. 18 Convergence of the plate fourth natural frequency.

the natural frequencies, a nonlinear static solution was computed and the resulting tangent stiffness for the converged solution was used to compute the natural frequencies. Also shown on the plots are the corresponding linear and nonlinear finite element results. It is obvious that the behavior of the dynamic results are similar to the static results in that the CRR in-plane eigenmodes case shows exceedingly slow convergence to the nonlinear finite element results. With 100 in-plane trial functions, the error in the first four natural frequencies is (mode 1 to mode 4) 51.7, 44.4, 32.6, and 19.1%. On the other hand, all four of the natural frequencies for the CRR out-of-plane eigenmodes case are within 3% of the nonlinear finite element solution with only 30 trial functions.

IV. Conclusions

In this work the convergence characteristics of the classical Rayleigh–Ritz solution of the nonlinear von Kármán plate equations are studied, with respect to the in-plane trial functions used, for the static deflection of a cantilever plate subjected to a static gravity load. Four in-plane trial function types were studied: 1) CRR in-plane eigenmodes, in-plane eigenmodes from a linear plane stress finite element model; 2) CRR polynomial, polynomial functions; 3) CRR transcendental, transcendental functions; and 4) CRR out-of-plane eigenmodes, out-of-plane eigenmodes as computed by a linear shell finite element model. In all four cases, the same 10 trial functions were used in the expansion of the out-of-plane displacement. Studying the out-of-plane w and in-plane v deflections for two different static gravity loadings (0.00078125 and 0.025 $\mathrm{m/s^2}$), it was noted that the CRR solution that used in-plane trial functions of types 2 and 4 showed much better convergence characteristics than the solutions from types 1 and 3. For the 0.00078125 $\mathrm{m/s^2}$ loading case, for which the finite element model gave a maximum normalized (by the thickness) out-of-plane deflection of $w/h = 0.396$, CRR solutions that used in-plane trial functions of types 2 and 4 gave solutions within 0.5% of the FEM solution when only three in-plane trial functions were used. On the other hand, CRR solutions that used

in-plane trial functions of types 1 and 3 had an error of 17% with five trial functions and 2.3% with 50 trial functions. For the 0.025 m/s^2 loading case, for which the FEM solution gave a w/h of 12.287, CRR solutions with in-plane trial functions of types 1 and 3 were within 1.0% of the FEM solution when only 21 trial functions were used in the solution. However, for CRR solutions that used trial functions of type 2 and 4 the error was still over 40% when more than 80 trial functions were used.

To explain the differences, the solutions were examined with respect to the satisfaction of the natural boundary conditions. Better satisfaction of the zero stress resultant boundary conditions along the free edges was noted for cases 2 and 4. Locking of the solution with respect to the number of in-plane degrees of freedom and the satisfaction of the Ny stress resultant boundary condition was shown for the CRR solution that used transcendental trial functions. Similar locking behavior was noted for the case that used in-plane eigenmodes as trial functions, as these eigenmodes approximately satisfy the linear stress resultant boundary conditions.

Dynamic results in the form of the loaded plate eigenvalues were also examined. The static deflection of a plate will cause a change in the model stiffness when geometric nonlinearity is considered. This in turn has an effect on model eigenvalues. It was shown that the first four eigenvalues are computed accurately, when compared with a nonlinear finite element solution, using a classic Rayleigh–Ritz solution that used in-plane trial functions of type 4 (see Figs. 15–18). For this case, the first four eigenvalues were within 3% of the finite element solution with only 30 in-plane trial functions used in the solution. However when type 1 trial functions were used, convergence of the eigenvalues to the nonlinear finite element solution was poor. With 100 in-plane trial functions, the error (when compared to the nonlinear finite element solution) in first four eigenvalues was 51.7, 44.4, 32.6, and 19.1%, respectively.

From the preceding analysis one may draw the following conclusion: For a CRR solution of the von Kármán plate equations to achieve adequate convergence, it is important to choose in-plane trial functions that *do not* satisfy, either exactly or approximately, the *linear* natural boundary conditions for same problem. This allows the CRR solution procedure to be able to use all of the in-plane degree of freedom to make the problem functional as small as possible.

References

[1] Rayleigh, L., *Theory of Sound*, Vol. 1, Dover, New York, 1945 (first American edition of 1894 edition).

[2] Ritz, W., "On a New Method for Solution of Certain Variational Problems in Mathematical Physics," *Journal for Pure and Applied Mathematics*, Vol. 135, 1909, pp. 1–61.

[3] Ritz, W., "Theorie der Transversalschwingungen einer quadratischen Platte mit freie Rändern," *Annalen der Physik*, Vol. 38, 1909, pp. 737–786.

[4] Meirovitch, L., and Kwak, M. K., "Convergence of the Classical Rayleigh-Ritz Method and the Finite Element Method," *AIAA Journal*, Vol. 28, No. 8, 1990, pp. 1509–1516.

[5] Chia, C., *Nonlinear Analysis of Plates*, McGraw–Hill, New York, 1980.

[6] Sathyamoorthy, M., "Nonlinear Vibration Analysis of Plates: A Review and Survey of Current Developments," *Applied Mechanics Reviews*, Vol. 40, 1987, pp. 1553–1561.

[7] Gordnier, R., and Fithen, R., "Coupling of a Nonlinear Finite Element Structural Method with a Navier-Stokes Solver," *Computers and Structures*, Vol. 81, No. 2, 2003, pp. 75–89.

[8] Dowell, E., "Nonlinear Oscillations of a Fluttering Plate," *AIAA Journal*, Vol. 4, No. 7, 1966, pp. 1267–1275.

[9] Dowell, E., "Nonlinear Oscillations of a Fluttering Plate, Part 2," *AIAA Journal*, Vol. 5, No. 10, 1967, pp. 1856–1862.

[10] Dowell, E., "Flutter of a Buckled Plate as an Example of Chaotic Motion of a Deterministic Autonomous System," *Journal of Sound and Vibration*, Vol. 85, No. 3, 1982, pp. 333–334.

[11] Bolotin, V., Grishko, A., Kounadis, A., and Gantes, C., "Influence of Initial Conditions on the Post-Critical Behavior of a Nonlinear Aeroelastic System," *Nonlinear Dynamics*, Vol. 15, No. 1, 1998, pp. 63–81.

[12] Bolotin, V., Grishko, A., Kounadis, A., and Gantes, C., "The Fluttering Panel as a Continuous Nonlinear Nonconservative System," *Journal of Vibration and Control*, Vol. 7, No. 2, 2001, pp. 233–247.

[13] Epureanu, B., Tang, L., and Paidoussis, M., "Coherent Structures and Their Influence on the Dynamics of Aeroelastic Panels," *International Journal of Non-Linear Mechanics*, Vol. 39, No. 6, Aug. 2004, pp. 977–991.

[14] Hopkins, M., "Nonlinear Response of a Fluttering Plate Subject to Supersonic Aerodynamic, Thermal, and Pressure Loads," Ph.D. Thesis, Duke Univ., Durham, NC, 1994.

[15] Tang, D., Henry, J., and Dowell, E., "Limit Cycle Oscillations of Delta Wing Models in Low Subsonic Flow," *AIAA Journal*, Vol. 37, No. 11, 1999, pp. 155–164.

[16] Tang, D., Dowell, E., and Hall, K., "Limit Cycle Oscillations of a Cantilevered Wing in Low Subsonic Flow," *AIAA Journal*, Vol. 37, No. 3, 1999, pp. 364–371.

[17] Tang, D., and Dowell, E., "Effects of Angle of Attack on Nonlinear Flutter of a Delta Wing," *AIAA Journal*, Vol. 39, No. 1, 2001, pp. 15–21.

[18] Attar, P., Dowell, E., and Tang, D., "Theoretical and Experimental Investigation of the Effects of a Steady Angle of Attack on the Nonlinear Flutter of a Delta Wing Plate Model," *Journal of Fluids and Structures*, Vol. 17, No. 2, 2003, pp. 243–259.

[19] Attar, P., Dowell, E., and White, J., "Modeling the LCO of a Delta Wing Using a High Fidelity Structural Model," *Journal of Aircraft*, Vol. 42, No. 5, Sept.–Oct. 2005, pp. 1209–1217.

[20] Attar, P. J., Dowell, E. H., White, J. R., and Thomas, J. P., "A Reduced Order Nonlinear System Identification Methodology," *AIAA Journal* (submitted for publication).

[21] Attar, P., and Gordnier, R., "Aeroelastic Prediction of the Limit Cycle Oscillations of a Cropped Delta Wing," *Journal of Fluids and Structures*, Vol. 21, No. 7, 2006, pp. 45–58.

[22] Gordnier, R., "Computation of Limit-Cycle Oscillations of a Delta Wing," *Journal of Aircraft*, Vol. 40, No. 6, 2003, pp. 1206–1207.

[23] Gordnier, R. E., and Visbal, M. R., "Numerical Simulation of Nonslender Delta Wing Buffet at High Angle of Attack," AIAA Paper 2004-2047, April 2004.

[24] Gordnier, R. E., and Visbal, M. R., "Computation of the Aeroelastic Response of a Flexible Delta Wing at High Angles of Attack," AIAA Paper 2003-1728, April 2003.

[25] Schairer, E., and Hand, L., "Measurement of Unsteady Aeroelastic Model Deformation by Stereo Photogrammetry," AIAA Paper 1997-2217, June 1997.

[26] Novzhilov, V., *Foundations of the Nonlinear Theory of Elasticity*, Dover, New York, 1953.

[27] Dowell, E., *Aeroelasticity of Plates and Shells*, Noordhoff International Publishers, Leiden, The Netherlands, 1975.

[28] Smith, S., Bradford, M., and Oehlers, D., "Numerical Convergence of Simple and Orthogonal Polynomials for the Unilateral Plate Buckling Problem Using the Rayleigh-Ritz Method," *International Journal for Numerical Methods in Engineering*, Vol. 44, No. 11, 1999, pp. 1685–1707.